Modelling and Simulation of DFIG-WT for Voltage Regulation

Youssef A. Mobarak, Mohamed I. Kamal, S. A. Deraz, M. El-Shahat Dessouki, A. El-Bahnasawy, Ahmed A. Abouelfadl, F. S. Elhosarey, A. I. Elbasiouny

Faculty of Engineering, King Abdulaziz University, Rabigh 21911, Saudi Arabia

Abstract— *Nowadays, wind energy is considered as one of the most developing and promising renewable energy sources. Because of power electronics advancements, wind energy conversion systems (WECSs) equipped with Doubly Fed Induction Generators (DFIGs) for variable speed wind turbines (VSWTs) are one of the most efficient topologies for WECS. Further, due to the merits of DFIG over other generators, it is involved in most of wind power applications. Therefore, modelling and simulation of DFIG coupled with VSWT has taken a great attention by researches. In this article, power generation control in variable-speed variable-pitch horizontal-axis wind turbines operating at high wind speeds is studied. Response of DFIG wind turbine system to grid disturbances is simulated. The simulation results show the effectiveness of the proposed controllers for power regulation and demonstrate high-performance. A dynamic chattering torque control and a proportional integral PI pitch control strategies are proposed and validated using MATLAB software program.*

Keywords - *Wind Turbine, Variable-Speed, Variable-Pitch, Voltage Regulation, DFIG.*

I. INTRODUCTION

Due to degradation of fossil fuels and global environmental concerns, a great focus on alternative methods of electricity generation is increased. Towards the energy market diversification, wind power is the fastest growing sustainable energy resource [1-5]. WTs with elementary control systems that aim to minimize cost and maintenance of the installation have predominated for a long time. Recently, the increasing size of the turbines and the greater penetration of wind energy into the electrical utilities have encouraged the use of power electronic converters and mechanical actuators. These active devices incorporate extra degrees of freedom into the design, allowing for active control of the captured power. Static power electronic converters, used as an interface to the grid, enable variable-speed operation of the wind turbine. Due to external perturbations, such as random wind fluctuations, wind shear and tower shadows, variable speed control seems to be a good option for optimizing the operation of wind turbines [2]. WECSs are challenging from the control system viewpoint. Wind turbines inherently exhibit nonlinear dynamics and are exposed to large cyclic disturbances that may excite the poorly damped vibration modes of the drive train and tower [1, 3]. In addition, it is difficult to derive mathematical models that accurately describe the dynamic behaviour of WTs because of the particular operating conditions. Moreover, this task is even more involved due to the current tendency towards larger and more flexible WTs. Lack of the accurate models of WTs is countered by robust control strategies that capable of securing stability and certain performance features despite model uncertainties. Problems of WTs control are become more challenging when WTs operated at variable-speed and variable-pitch [4–6]. The best use of this type of turbine can only be achieved with several controllers [7, 8]. WTs can operate either at fixed speed or at variable speed. For a fixed speed wind turbine (FSWT), the generator is directly connected to the electrical grid. For a variable speed wind turbine (VSWT), the generator is controlled by power electronic equipment. There are several reasons for using VSWTs; among them are the possibilities to reduce the mechanical stresses and acoustic noise and to control the active and reactive powers. Most manufactures of WTs are developing new large WTs in the range of 3-5 MW. These large WTs operate on variable-speed with pitch control using a direct driven synchronous generator (without gearbox) or DFIG. Fixed-speed induction generators with stall control are regarded as unfeasible for these large WTs. DFIGs are commonly used by the wind turbine industry for larger wind turbines [8-14], because of the rotor power of the induction generator depends on the slip and at the same time the power from the rotor is not wasted as in the case of induction machines with external variable rotor resistance. But it is fed to the grid, so varying the slip of the generator doesn't lower the efficiency any more. The system needs a converter, and unfortunately a complicated control system adjusting the slip to the given rotor speed. Therefore, the overall system efficiency is improved in comparison with fixed-speed generators.

In addition, the use of DFIGs for VSWTs offers other advantages regarding the power electronic devices connected together [11]. The cost of power electronic converter is reduced because its low required converter power rating. The converter has to deal only with approximately 25% of the total power of the generator because the main part of the

energy passes from the stator directly to the grid. Therefore the required converter can be rated at a quarter of the total system power [12]. Also the cost of the converter filters and EMI filters are lower. The power-factor control can be implemented at lower cost, because the four-quadrant converter together with the induction machine basically operates similar to a synchronous generator. So, the converter has to provide only the excitation energy. Another important advantage of the above presented scheme is that the four-quadrant converter in the rotor circuit enables decoupled control of active and reactive power of the generator.

In this article, a new control strategy for variable-speed variable-pitch horizontal-axis wind turbine (HAWT) is proposed. The proposed control strategy is obtained with a nonlinear dynamic chattering torque control and a proportional integral (PI) control for the blade pitch angle. The proposed strategy allows for a rapid transition of the WT generated power between different desired values. This implies that it is possible to increase or decrease the WT power production with consideration of the power consumption on the utility grid. This electrical power tracking is ensured with high-performance behaviours for all other state variables: including turbine and generator rotational speeds; and smooth and adequate evolution of the control variables. The DFIG coupled with WT for voltage, and var regulation control is modelled and simulated. System response to a change in wind speed, voltage sag on the 120kV system and single line fault on the 25kV system are discussed in this study.

II. System Modelling

A. Wind Turbine

The WT consists of a rotor assembly, gear-box, and generator. Rotor of WT extracts the energy from the wind and converts it into mechanical power. A simplified model of the rotor was presented in [15–17] as:

$$P_m = \frac{1}{2} c_p(\lambda,\beta)\rho\pi R^2 v_w^3 \quad (1)$$

Where ρ defines the air density, R is the radius of the rotor, v_w is the wind speed, c_p is the power coefficient of the WT, β is the pitch angle, and λ is the tip-speed ratio given by:

$$\lambda = \frac{R\omega_r}{v_w} \quad (2)$$

Therefore, changes in the wind speed or rotor speed produce changes in the tip-speed ratio, leading to power coefficient variation, so, the power generated is affected. The aerodynamic torque coefficient is related to the power coefficient as follows:

$$P_m = \omega_r T_a \quad (3)$$

The aerodynamic torque expression is described as:

$$T_a = \frac{1}{2} c_q(\lambda,\beta)\rho\pi R^3 v_w^2 \quad (4)$$

$$c_q(\lambda,\beta) = \frac{c_p(\lambda,\beta)}{\lambda} \quad (5)$$

For a perfectly rigid low-speed shaft, a single-mass model for a wind turbine can be considered as [18–21]:

$$J_t\dot{\omega}_r = T_a - K_t\omega_r - T_g \quad (6)$$

Where J_t is the turbine total inertia (kg-m^2), K_t is the turbine total external damping (Nm rad^{-1} s), T_a is the aerodynamic torque (N.m), and T_g is the generator torque (N.m). The scheme of the one-mass model is provided in Fig. 1. The model is based on the steady-state power characteristics of the turbine. The stiffness of the drive train is infinite and the friction factor and the inertia of the turbine must be combined with those of the generator coupled to the turbine. A generic equation is used to model $c_p(\lambda,\beta)$. This equation, based on the modelling turbine characteristics of [1], is given as:

$$c_P(\lambda,\beta) = c_1\left(\frac{c_2}{\lambda_i} - c_3\beta - c_4\right)e^{-c_5/\lambda_i} + c_6\lambda \quad (7)$$

With: $\frac{1}{\lambda_i} = \frac{1}{\lambda+0.08\beta} - \frac{0.035}{\beta^3+1}$

Where c_1 to c_6 are constant coefficients and given as: $c_1 = 0.5176$, $c_2 = 116$, $c_3 = 0.4$, $c_4 = 5$, $c_5 = 21$ and $c_6 = 0.0068$. The c_p-λ characteristics, for different values of the pitch angle β, are illustrated in Fig. 2. The maximum value of c_p ($c_{pmax} = 0.48$) is achieved for β = 0 degree and for λ = 8.1. This particular value of λ is defined as the nominal value (λ_{nom}). Fig. 3 shows wind turbine power characteristics. Pitch angle β is used to display the power characteristics. Beta must be greater than or equal to zero. The mechanical power Pm as a function of generator speed, for different wind speeds and for blade pitch angle β = 0 degree. This figure is obtained with the default parameters (base wind speed = 12 m/s, maximum power at base wind speed = 0.73 pu (k_p = 0.73) and base rotational speed = 1.2 pu).

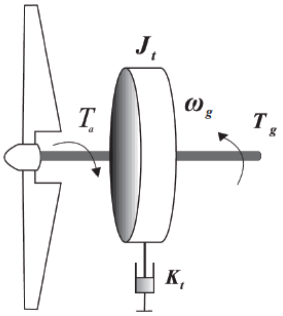

Fig. 1 One-mass model of a wind turbine

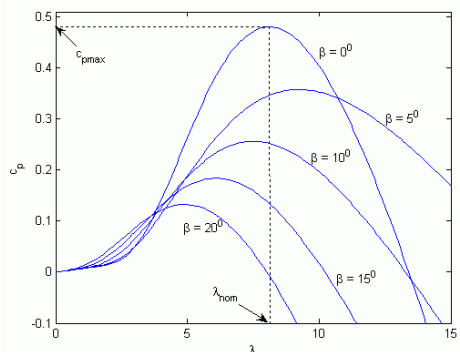

Fig. 2 c_p-λ characteristics for different values of the pitch angle β

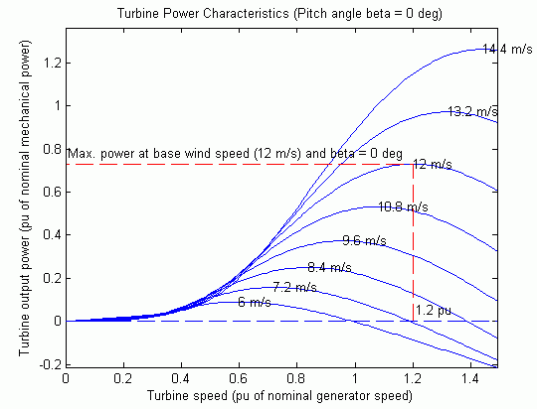

Fig. 3 Wind turbine power characteristics

B. Wind Turbine Induction Generator

Wind turbine induction generator (WTIG) system is shown in Fig. 4. The stator winding is connected directly to the grid and the rotor is driven by the wind turbine. The power captured by the wind turbine is converted into electrical power by the induction generator and is transmitted to the grid by the stator winding. For high wind speeds, the pitch angle is controlled to limit the output power of the generator to its nominal value. In order to generate power the induction generator speed must be slightly above the synchronous speed. But the speed variation is typically so small that the WTIG is considered to be a fixed-speed wind generator. The var power absorbed by the induction generator is provided by the grid or by some devices like capacitor banks, SVC, STATCOM or synchronous condenser [22-25].

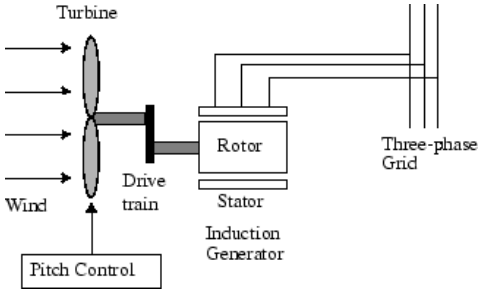

Fig. 4 WTIG system

C. Wind Turbine Doubly-Fed Induction Generator WT-DFIG

Efficient wind power plants use variable-speed generators for electrical generation [22]. There are several advantages of using such generators [23]. They can reduce mechanical stresses by storing the energy from windstorm in the mechanical inertia of the turbine, creating a sort of elasticity that reduces torque pulsations and improve the power quality. The system efficiency can be slightly improved by adjusting the turbine speed to maximize output power. The applied converters can also supply reactive power to the grid if the converters are rated for this purpose [24]. Several types of adjustable-speed generators are used for such purposes [25]. The most common one is the DFIG. Practically, the stator of the DFIG is connected directly, or through a three phase transformer to the grid. The rotor windings are coupled by slip rings to the same grid through a four-quadrant AC-AC converter as shown in Fig. 5 [26]. The AC/DC/AC converter is divided into two components: the rotor-side converter C_{rotor} and the grid-side converter C_{grid}. Both converters are voltage-source converters (VSCs) that use forced-commutated power electronic devices IGBTs to synthesize an AC voltage from a DC voltage source. A capacitor connected on the DC side acts as the DC voltage source. A coupling inductor L is used to connect C_{grid} to the grid. The three-phase rotor winding is connected to C_{rotor} by slip rings and brushes and the three-phase stator winding is directly connected to the grid. The power captured by the wind turbine is converted into electrical power by the induction generator and it is transmitted to the grid by the stator and the rotor windings. The control system generates the pitch angle command and the voltage command signals V_r and V_{gc} for C_{rotor} and C_{grid} respectively in order to control the power of the wind turbine, the DC bus voltage and the reactive power or the voltage at the grid terminals. The power flow, illustrated in the Fig. 6, is used to describe the operating principle [27-30].

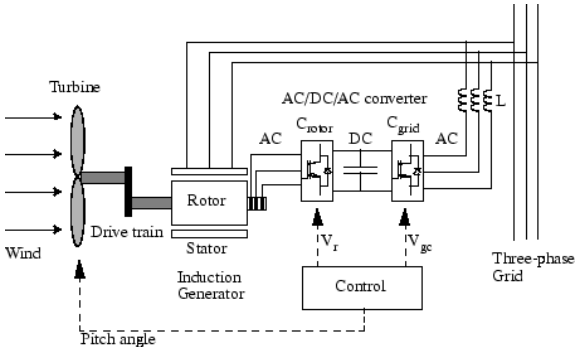

Fig. 5 WT-DFIG system

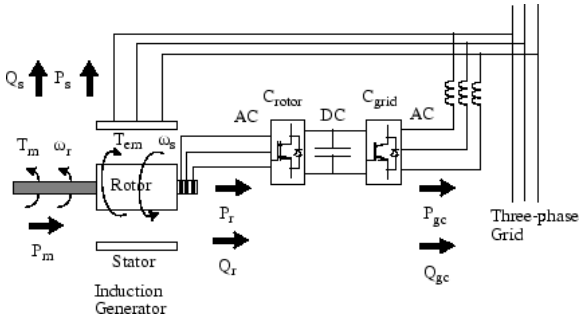

Fig. 6 WT-DFIG power flow

The mechanical power and the stator electric power output are computed as follows:

$$P_m = T_m \omega_r P_s = T_{em} \omega_s \quad (8)$$

For a lossless generator the mechanical equation is:

$$J \frac{d\omega_r}{dt} = T_m - T_{em} \quad (9)$$

In steady-state at fixed speed for a lossless generator Tm = Tem and Pm = Ps + Pr. It follows as:

$$P_r = P_m - P_s = T_m \omega_r - T_{me} \omega_s = -T_m \frac{\omega_s - \omega_r}{\omega_s} \omega_s$$
$$= -sT_m \omega_s = -sP_s \quad (10)$$

Where s is defined as the slip of the generator; s = (ωs–ωr)/ωs.

Generally the absolute value of slip is much lower than unity and, consequently, P_r is only a fraction of Ps. Since Tm is positive for power generation and since ω_s is positive and constant for a constant frequency grid voltage, the sign of P_r is a function of the slip sign. P_r is positive for negative slip and it is negative for positive slip. For super-synchronous speed operation, P_r is transmitted to DC bus capacitor and tends to rise the DC voltage. For sub-synchronous speed operation, P_r is taken out of DC bus capacitor and tends to decrease the DC voltage. C_{grid} is used to generate or absorb the power P_{gc} in order to keep the DC voltage constant. In steady-state for a lossless AC/DC/AC converter P_{gc} is equal to P_r and the speed of the wind turbine is determined by the power P_r absorbed or generated by C_{rotor}. The phase-sequence of the AC voltage generated by C_{rotor} is positive for sub-synchronous speed and negative for super-synchronous speed. The frequency of this voltage is equal to the product of the grid frequency and the absolute value of the slip. C_{rotor} and C_{grid} have the capability of generating or absorbing reactive power and could be used to control the reactive power or the voltage at the grid terminals [31-33].

The actual electrical output power is illustrated in the Fig. 7, measured at the grid terminals of the wind turbine, is added to the total power losses and is compared with the reference power obtained from the tracking characteristic. A Proportional-Integral PI regulator is used to reduce the power error to zero. The output of this regulator is the reference rotor current I_{qr_ref} that must be injected in the rotor by converter C_{rotor}. This is the current component that produces the electromagnetic torque T_{em}. The actual I_{qr} component of positive-sequence current is compared to I_{qr_ref} and the error is reduced to zero by a current regulator PI. The output of this current controller is the voltage V_{qr} generated by C_{rotor}. The current regulator is assisted by feed forward terms which predict V_{qr}. The voltage or the reactive power at grid terminals is controlled by the reactive current flowing in the converter C_{rotor}. As long as the reactive current stays within the maximum current values ($-I_{max}$, I_{max}) imposed by the converter rating, the voltage is regulated at the reference voltage V_{ref}. However, a voltage droop is normally used (usually between 1% and 4% at maximum reactive power output), and the V-I characteristic has the slope indicated in the Fig. 8 [34-36].

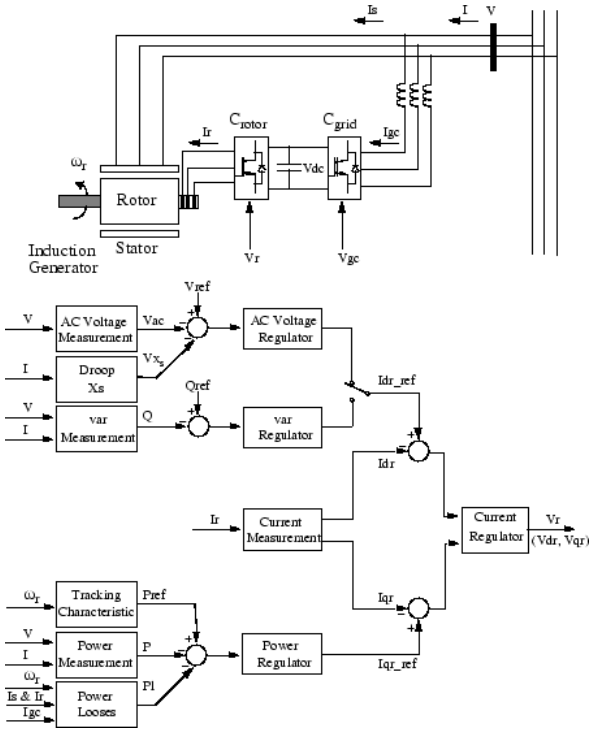

Fig. 7 Rotor-side converter control system

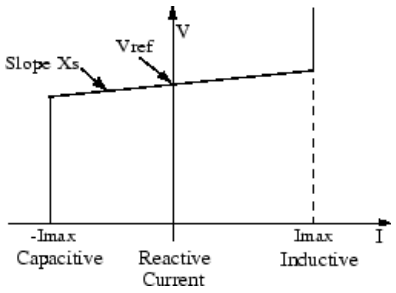

Fig. 8 Wind turbine V-I characteristic

In the voltage regulation mode, the V-I characteristic is described by the following equation:

$$V = V_{ref} - X_s I \quad (11)$$

The output of the voltage regulator or the var regulator is the reference d-axis current I_{dr_ref} that must be injected in the rotor by converter Crotor.

The same current regulator as for the power control is used to regulate the actual I_{dr} component of positive-sequence current to its reference value. The output of this regulator is the d-axis voltage V_{dr} generated by C_{rotor}. The current regulator is assisted by feed forward terms which predict V_{dr}. The converter C_{grid} is used to regulate the voltage of the DC bus capacitor. In addition, this model allows using C_{grid} converter to generate or absorb reactive power. The control system is illustrated in Fig. 9. The maximum value of this current is limited to a value defined by the converter maximum power at nominal voltage. When I_{dgc}_ref and I_{q_ref} are such that the magnitude is higher than this maximum value the I_{q_ref} component is reduced in order to bring back the magnitude to its maximum value [34-36].

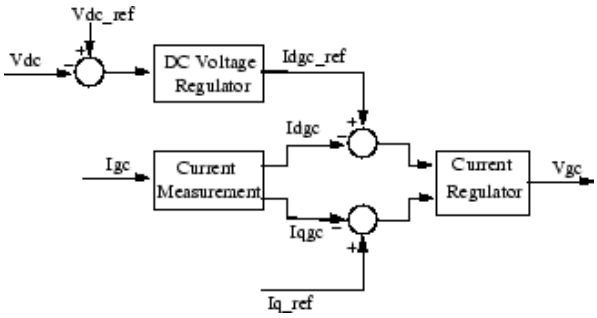

Fig. 9 Grid-Side Converter Control System

D. Pitch Angle Control System

To assist the torque controller with regulating the wind turbine electric power output, while avoiding significant loads and maintaining the rotor speed within acceptable limits, a pitch proportional integral PI controller is added to the rotor speed tracking error. A PI controller is used to control the blade pitch angle in order to limit the electric output power to the nominal mechanical power. The pitch angle is kept constant at zero degree when the measured electric output power is under its nominal value. When it increases above its nominal value the PI controller increases the pitch angle to bring back the measured power to its nominal value [37]. The control system is illustrated in the Fig. 10:

$$\beta = K_P(\omega_r - \omega_n) + K_i \int_0^t (\omega_r - \omega_n)dt,$$
$$\text{and } K_p > 0;\ K_i > 0 \qquad (12)$$

Where ω_r is the rotor speed and ω_n is the nominal rotor speed, at which the rated electrical power of the wind turbine is obtained. To disable the proportional term when $\omega_r < \omega_n$, the final proposed controller is described with the following expression as:

$$\beta = \frac{1}{2}K_P(\omega_r - \omega_n)\big(1 + sgn(\omega_r - \omega_n)\big) + K_i \int_0^t (\omega_r - \omega_n)dt, \text{ and } K_p > 0 \qquad (13)$$

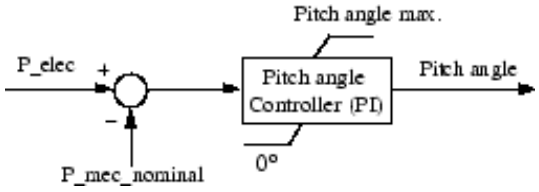

Fig. 10 Pitch angle control system

III. The Mathematical Model of the DFIG

In general terms simulations are helpful in gaining insights to the dynamic behaviour of any electrical drive system. They offer a fast and economical means by which they can conduct studies to learn more about these components [13]. The main goal of our research was to study the decoupled control of active and reactive power in wind power plants having doubly fed induction generators. This practically could not be performed without high performance simulation programs. The first step towards the dynamic simulations was to build up the mathematical model of the doubly fed induction generator. The widely used dq reference frame was chosen to model the generator. In this case both the three-phased stator and rotor symmetrical windings are transformed in orthogonal two axis systems upon Park's transformation. Hence the model machine has only 4 windings (two on the stator and two on the rotor) in quadrature. The fixed reference frame was selected for writing the equations. The angular speed of the reference frame in this case will be:

$$\omega_c = 0 \qquad (14)$$

For the stator windings the generator convention will be used, and for rotor windings the load one [14]. The saturation effect of the magnetic cores also will be taken into account. Using the above conditions the following set of voltage equations results for the four windings as:

$$V_d = -R_s i_d - \frac{d\lambda_d}{dt}, \text{ and } V_q = -R_s i_q - \frac{d\lambda_q}{dt} \qquad (15)$$

$$V_D = R_r i_D + \frac{d\lambda_D}{dt} + \omega\lambda_Q, \text{ and } V_Q = R_r i_Q + \frac{d\lambda_Q}{dt} - \omega\lambda_D \qquad (16)$$

The d and q indices indicate the direct and quadrature axis components, respectively. With uppercase are marked the rotor quantities. The s and r indices refer to the stator and rotor quantities, respectively. It should be mentioned that all the rotor quantities are referred to the stator of the machine. To be able to solve the problem another set of equations is required, the flux-current equations, written also for the four windings:

$$\lambda_d = L_{r\sigma} i_d + M(i_d + i_D), \text{ and } \lambda_q = L_{s\sigma} i_q + M\big(i_q + i_Q\big) \qquad (17)$$

$$\lambda_D = L_{r\sigma} i_D + M(i_d + i_D) \quad , \quad \text{and} \quad \lambda_Q = L_{r\sigma} i_Q + M\big(i_q + i_Q\big) \qquad (18)$$

Where $L_{s\sigma}$ and $L_{r\sigma}$ are the leakage inductances, respectively $M = M_d = M_q$ is the main magnetizing inductance. The mathematical model of the generator must be completed by to equations due to the load connected on its terminals:

$$V_d = R_l i_{ld} + L_l \frac{di_{ld}}{dt} \text{and}$$
$$V_q = R_l i_{lq} + L_l \frac{di_{lq}}{dt} \quad (19)$$

Where R_l and L_l are the resistance and inductance of the load, respectively i_{ld} and i_{lq} are the two orthogonal components of the load current. The saturation effect of the non-linear iron cores is taken into account by defining a transient (dynamic) magnetizing inductance, $M_t = d\lambda_m/di_m$, being function of the magnetizing current. Finally the mathematical model of the DFIG will be obtained by substituting equations (17), (18) in the voltage equations (15), (16):

$$V_d = -R_s i_d - L_{s\sigma} \frac{di_d}{dt} - M_t \left(\frac{di_d}{dt} + \frac{di_D}{dt}\right) \quad (20)$$
$$V_q = -R_s i_q - L_{s\sigma} \frac{di_q}{dt} - M_t \left(\frac{di_q}{dt} + \frac{di_Q}{dt}\right) \quad (21)$$
$$V_D = R_r i_D + L_{r\sigma} \frac{di_q}{dt} + M_t \left(\frac{di_d}{dt} + \frac{di_D}{dt}\right) + \omega L_{r\sigma} i_Q + M\omega\left(i_q + i_Q\right) \quad (22)$$
$$V_Q = R_r i_Q + L_{r\sigma} \frac{di_Q}{dt} + M_t \left(\frac{di_q}{dt} + \frac{di_Q}{dt}\right) - \omega L_{r\sigma} i_D - M\omega(i_d + i_D) \quad (23)$$

These equations must be transformed in a way to be in a practical form for implementing in any simulation environment: Equations (24), (27) together with the equations of the load (19) form together the mathematical model of the DFIG, which was used in our simulations.

$$\frac{di_d}{dt} = \frac{-V_d(L_{r\sigma}+M_t) - M_t V_D - R_s(L_{r\sigma}+M_t) i_d + \omega M M_t i_q + R_r M_t i_D + \omega M_t (L_{r\sigma}+M) i_Q}{L_{s\sigma} L_{r\sigma} + L_{s\sigma} M + L_{r\sigma} M} \quad (24)$$

$$\frac{di_q}{dt} = \frac{-V_q(L_{r\sigma}+M_t) - M_t V_Q - R_s(L_{r\sigma}+M_t) i_q - \omega M M_t i_d + R_r M_t i_Q - \omega M_t (L_{r\sigma}+M) i_D}{L_{s\sigma} L_{r\sigma} + L_{s\sigma} M + L_{r\sigma} M} \quad (25)$$

$$\frac{di_D}{dt} = \frac{V_d M_t + (L_{s\sigma}+M_t) V_D + R_s M_t i_d - R_r (L_{s\sigma}+M_t) i_D - \omega M (L_{s\sigma}+M_t) i_q - \omega (L_{s\sigma}+M_t)(L_{R\sigma}+M) i_Q}{L_{s\sigma} L_{r\sigma} + L_{s\sigma} M + L_{r\sigma} M} \quad (26)$$

$$\frac{di_Q}{dt} = \frac{V_q M_t + (L_{s\sigma}+M_t) V_Q + R_s M_t i_q - R_r (L_{s\sigma}+M_t) i_Q + \omega M (L_{s\sigma}+M_t) i_d + \omega (L_{s\sigma}+M_t)(L_{r\sigma}+M) i_D}{L_{s\sigma} L_{r\sigma} + L_{s\sigma} M + L_{r\sigma} M} \quad (27)$$

IV. STUDIED SYSTEM

Fig. 11 illustrates the performance of a 9 MW wind farm connected to a distribution system. The wind farm consists of six 1.5 MW wind turbines connected to a 25 kV distribution system exporting power to a 120 kV grid through a 30 km, and 25 kV feeder. A 2.3 kV, 2 MVA plant consisting of a motor load (1.68 MW induction motor at 0.93 power factor) and of a 200 kW resistive load is connected on the same feeder at bus 25 kV. A 500 kW load is also connected on the 575 V bus of the wind farm.

Both the wind turbine and the motor load have a protection system monitoring voltage, current and machine speed. The dc link voltage of the DFIG is also monitored. Wind turbines use a DFIG consisting of a wound rotor induction generator and an AC/DC/AC IGBT-based PWM converter. The stator winding is connected directly to the 60Hz grid while the rotor is fed at variable frequency through the AC/DC/AC converter. The DFIG technology allows extracting maximum energy from the wind for low wind speeds by optimizing the turbine speed, while minimizing mechanical stresses on the turbine during gusts of wind. The optimum turbine speed producing maximum mechanical energy for a given wind speed is proportional to the wind speed. Another advantage of the DFIG technology is the ability for power electronic converters to generate or turbine and the turbine power characteristics absorb reactive power, thus eliminating the need for installing capacitor banks as in the case of squirrel-cage induction generators. In this case study, the rotor is running at sub-synchronous speed for wind speeds lower than 10m/s and it is running at a super-synchronous speed for higher wind speeds. The turbine mechanical power as function of turbine speed is displayed in for wind speeds ranging from 5 m/s to 16.2 m/s. These characteristics are obtained with the specified parameters of the turbine characteristics as shown in Fig. 12. The power is controlled in order to follow a pre-defined power-speed characteristic, named tracking characteristic. Fig. 12 shows the turbine and tracking characteristic, by the ABCD curve superimposed to the mechanical power characteristics of the turbine obtained at different wind speeds. The actual speed of the turbine ωr is measured and the corresponding mechanical power of the tracking characteristic is used as the reference power for the power control loop. The tracking characteristic is defined by four points: A, B, C and D. From zero speed to speed of point A the reference power is zero. Between point A and point B the tracking characteristic is a straight line, the speed of point B must be greater than the speed of point A. Between point B and point C the tracking characteristic is the locus of the maximum power of the turbine. The tracking characteristic is a straight line from point C and point D. The power at point D is 1.0 pu and the speed of the point D must be greater than the speed of point C. Beyond point D the reference power is a constant equal to 1.0 pu [37].

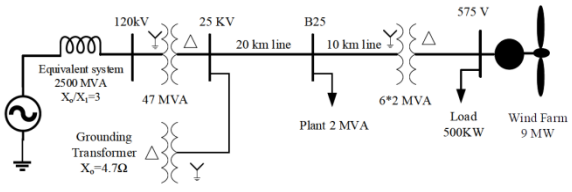

Fig. 11 Single-line diagram of the wind farm connected to a distribution system

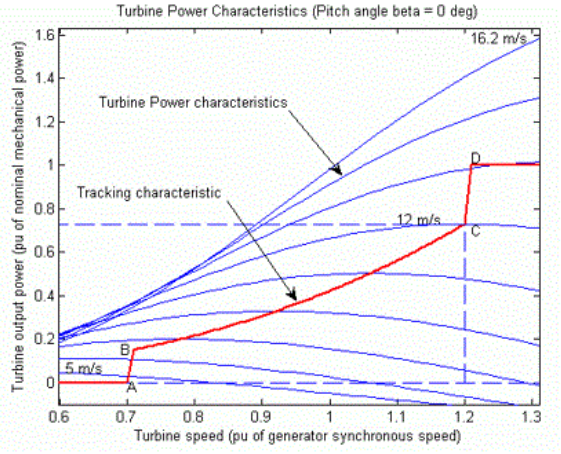

Fig. 12 Turbine power characteristics

V. Results and Discussions

A. *Turbine Response to a Change in Wind Speed*

Initially, wind speed is set at 8 m/s, and then at t= 5s, wind speed increases suddenly at 14 m/s. Waveforms for a Gust of wind for voltage regulation illustrates in Fig. 13. At t= 5s, the generated active power starts increasing smoothly (together with the turbine speed) to reach its rated value of 9MW in approximately 15 s. Over that time frame the turbine speed increases from 0.8pu to 1.21pu. Initially, the pitch angle of the turbine blades is zero degree and the turbine operating point follows the red curve of the turbine power characteristics up to point D. Then the pitch angle is increased from 0o to 0.76o to limit the mechanical power. Observe also the voltage and the generated reactive power. The reactive power is controlled to maintain a 1.0pu voltage. At nominal power, the wind turbine absorbs 0.68Mvar to control voltage at 1.0 pu. While, for var regulation with the generated reactive power Q_{ref} set to zero, you will observe that the voltage increases to 1.021pu when the wind turbine generates its nominal power at unity power factor as shown in Fig. 14.

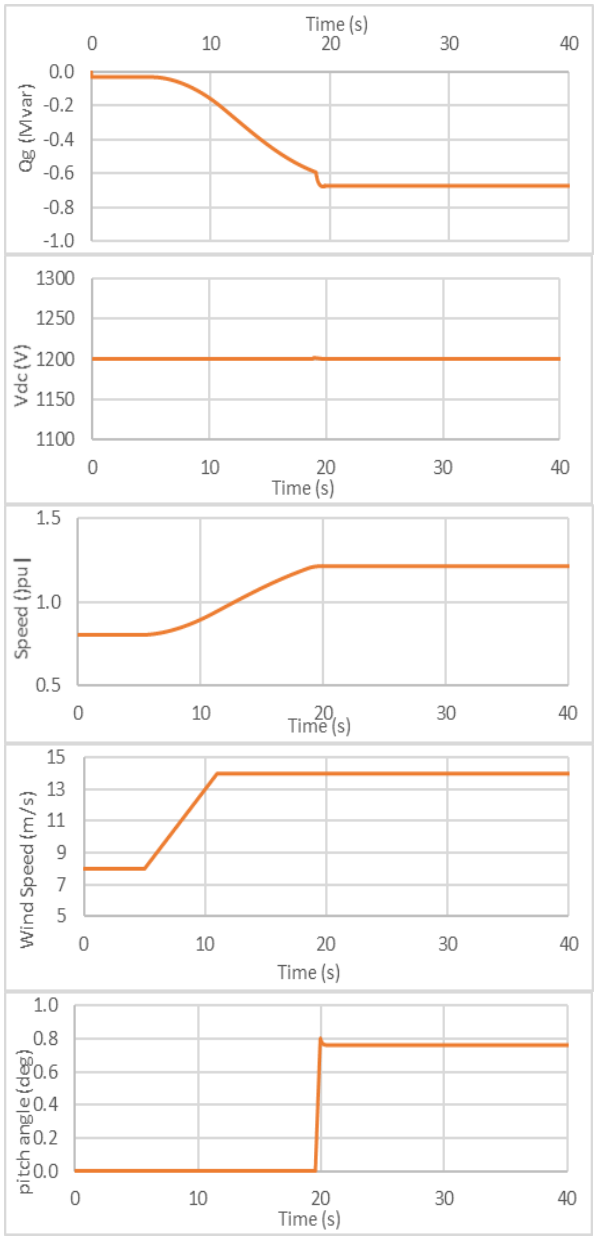

Fig. 13 Turbine response to a change in wind speed for voltage regulation

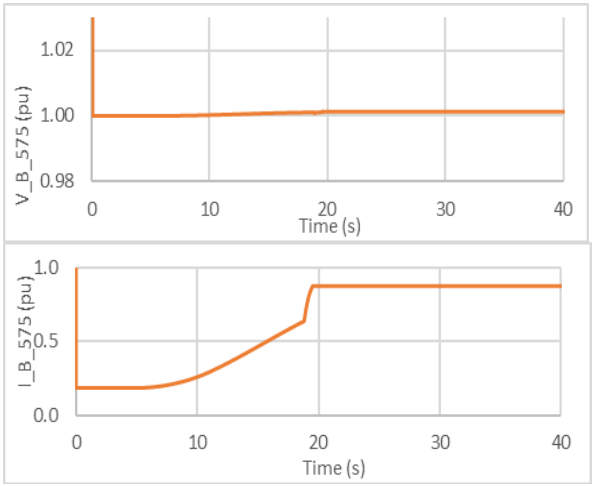

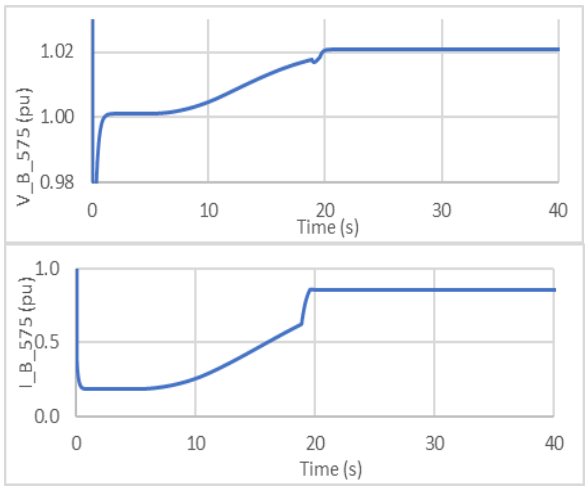

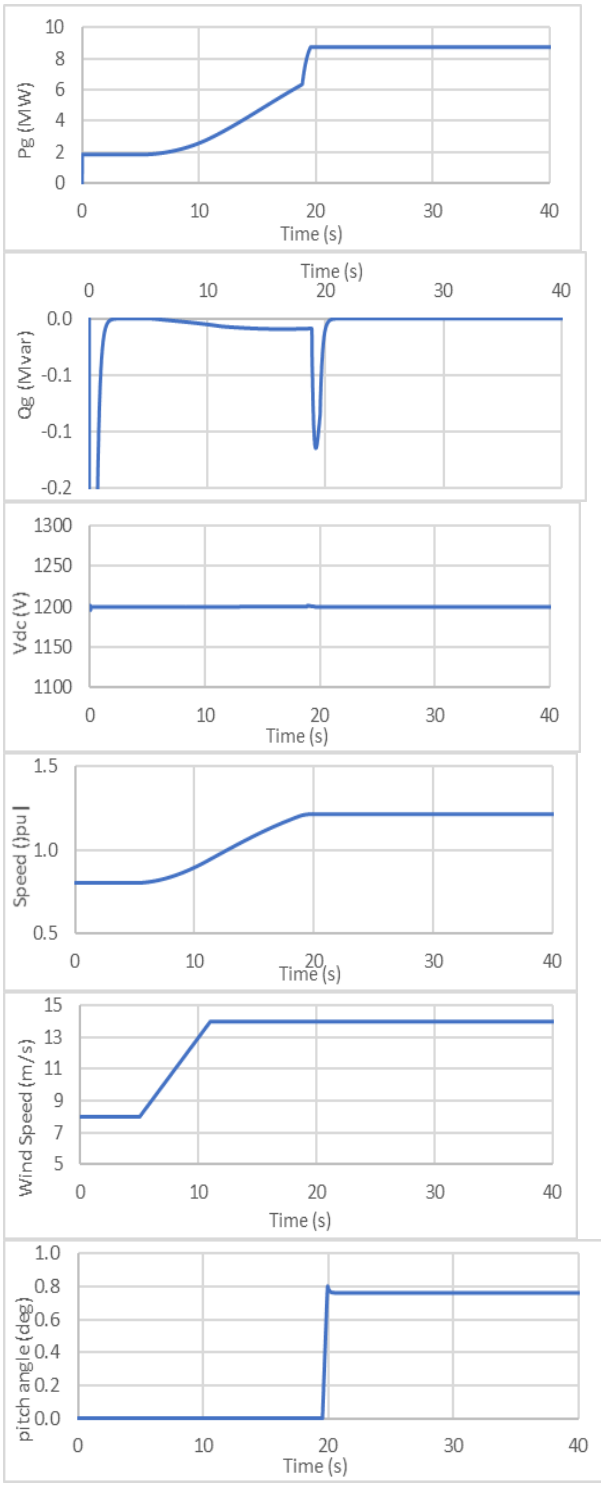

Fig. 14 Turbine response to a change in wind speed for var regulation

B. Simulation of a Voltage Sag on the 120 kV System

Now observe the impact of voltage sag resulting from a remote fault on the 120 kV system. In this simulation the mode of operation is initially var regulation with Q_{ref}=0 and the wind speed is constant at 8 m/s. A 0.15 pu voltage drop lasting 0.5 s is programmed, in the 120 kV voltage source menu, to occur at t= 5s. The simulation results are illustrated in voltage sag on the 120 kV system for wind farm in var regulation. Observe the plant voltage and current as well as the motor speed. Note that the wind farm produces 1.87 MW. At t= 5 s, the voltage falls below 0.9 pu and at t= 5.22 s, the protection system trips the plant because an under-voltage lasting more than 0.2 s has been detected (exceeding protection settings for the plant subsystem). The plant current falls to zero and motor speed decreases gradually, while the wind farm continues generating at a power level of 1.87 MW. After the plant has tripped, 1.25 MW of power is exported to the grid. Now, the wind turbine control mode is changed to voltage regulation and the simulation is repeated. You will notice that the plant does not trip anymore. This is because the voltage support provided by the 5 Mvar reactive power generated by the wind turbines during the voltage sag keeps the plant voltage above the 0.9 pu protection threshold. The plant voltage during the voltage sag is now 0.93 pu voltage sag on the 120 kV system wind farm in voltage regulation.

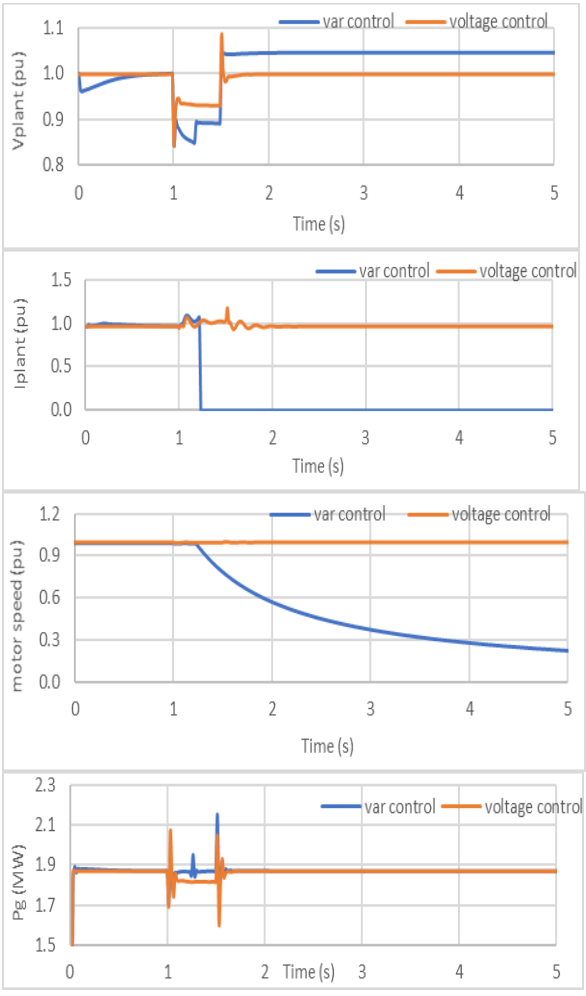

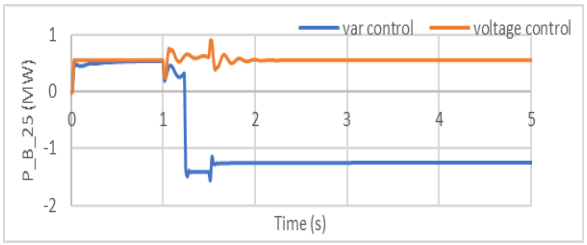

Fig. 15 Voltage sag on the 120 kV system for wind farm in var, and voltage regulation

C. Simulation of a Fault on the 25 kV System

Finally, now observe the impact of a single phase-to-ground fault occurring on the 25 kV line. At t=1.0 s a 9 cycle phase-to-ground fault is applied on phase A at 25kV bus. When the wind turbine is in voltage regulation, the positive sequence voltage at wind turbine terminals drops to 0.8 pu during the fault, which is above the under-voltage protection threshold (0.75 pu for a t > 0.1 s). The wind farm therefore stays in service as shown in Fig. 16. However, if the var regulation mode is used with Qref=0, the voltage drops under 0.7 pu and the under-voltage protection trips the wind farm. We can now observe that the turbine speed increases. At t=40 s the pitch angle starts to increase to limit the speed.

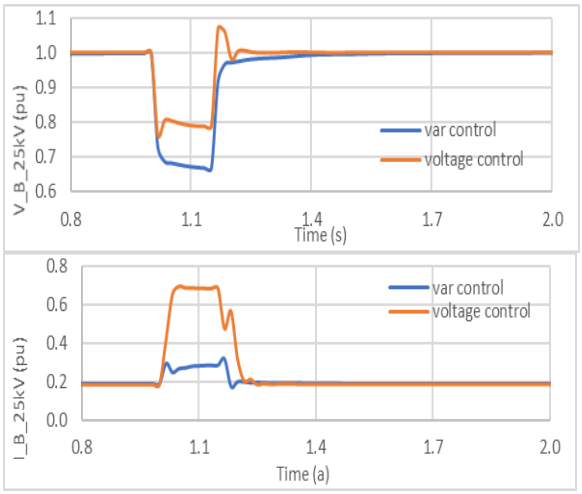

Fig. 16 Wind farm waveforms during fault at bus 25kV

VI. CONCLUSIONS

Due to its many advantages, the variable-speed wind turbine connected to DFIG is studied in this article. The system under study is modelled and simulated using MATLAB software program. A control strategy of DFIG-WT system is proposed. The proposed control strategy ensures the independent control of the active and reactive power generated by the induction generator. WT controller under turbulent wind conditions is presented. The proposed controller achieves strong performances in rotor speed and electrical power regulation with acceptable control activity. The results show that the proposed controller allows the WT generated power to transit between different desired set values. This achievement implies that it is possible to increase or decrease the WT power production in response to the power consumption of the network and to participate in the primary grid frequency control, which allows for a higher level of wind penetration in electric networks without affecting the quality of the generated electric power. Further, compared to other strategies, the advantages of the proposed controller are presented.

REFERENCES

[1] Burton, T., Sharpe, D., Jenkins, N., Bossanyi, E., *Wind Energy Handbook*, Wiley: Chichester, UK, 2001.

[2] Beaty, H.W., *Handbook of Electric Power Calculations*, 3rd ed., McGraw-Hill: New York, NY, USA, 2001.

[3] Spong, M.W., Vidyasagar, M., *Robot Dynamics and Control*, John Wiley and Sons: Hoboken, NJ, USA, 1989.

[4] Malcolm, D.J., Hansen, A.C., "Wind PACT Turbine Rotor Design Study", NREL/SR National Renewable Energy Laboratory: Golden, CO, USA, 2002.

[5] Siegfried Heier, *Grid Integration of Wind Energy Conversion Systems*, John Wiley & Sons Ltd, 1998.

[6] Johnson, G.L., *Wind Energy Systems*, Electronic Edition, Manhattan (USA), 2004.

[7] R. Pena, J.C. Clare, G.M. Asher, "Doubly fed induction generator using back-to-back PWM converters and its application to variable-speed wind-energy generation," *IEEE Proc.-Electrical Power Applied*, vol. 143, no. 3, May 1996.

[8] Zinger, D., Muljadi, E., "Annualized wind energy improvement using variable speeds," *IEEE Trans. Ind. Appl*., vol. 33, pp. 1444–1447, 1997.

[9] Boukhezzar, B., Lupu, L., Siguerdidjane, H., Hand, M., "Multivariable control strategy for variable speed, variable pitch wind turbines," *Renew. Energy*, vol. 32, pp. 1273–1287, 2007.

[10] De Battista, H.; Puleston, P.; Mantz, R.; Christiansen, C. "Sliding mode control of wind energy systems with DOIG-power efficiency and torsional dynamics optimization," *IEEE Trans. Power Systems*, 15, 728–734, 2000.

[11] Song, Y.; Dhinakaran, B.; Bao, X. "Variable speed control of wind turbines using nonlinear and adaptive algorithms," *J. Wind Eng. Ind. Aerodyn*., 85, 293–308, 2000.

[12] Slootweg, J., Polinder, H., Kling, W., "Dynamic Modelling of a Wind Turbine with Doubly Fed Induction Generator," *In Proceedings of the Power Engineering Society Summer Meeting*, July 2001,vol. 1, p. 644.

[13] Manjock, A. "Design Codes FAST and ADAMS for Load Calculations of Onshore Wind Turbines," National Renewable Energy Laboratory (NREL): Golden, CO, USA, 2005.

[14] Bhat, S.; Bernstein, D. Finite-Time Stability of Homogeneous Systems. *In Proceedings of the American Control Conference*, June 1997; vol. 4, pp. 2513–2514.

[15] Wu, B.; Bodson, M. "Direct adaptive cancellation of periodic disturbances for multivariable plants," *IEEE Trans. Speech Audio Process*., pp. 538–548, 2003.

[16] Ong, C.-M., *Dynamic Simulation of Electric Machinery Using Matlab/Simulink*, Prentice Hall PTR, Upper Saddle River (USA), 1997.

[17] Müller, S., Deicke, M., and de Doncker, R.W., "Doubly Fed Generator Systems for Wind Turbines," *IEEE Industry Applications Magazine*, pp. 26-33, May-June 2002.

[18] Vladislav Akhmatov, *Variable-Speed Wind Turbines with Doubly-Fed Induction Generators, Part I: Modelling in Dynamic Simulation Tools*, Wind Engineering, vol. 26, no. 2, 2002.

[19] Nicholas W. Miller, Juan J. Sanchez-Gasca, William W. Price, Robert W. Delmerico, "Dynamic Modeling of GE

1.5 and 3.6 Mw Wind Turbine-Generators For Stability Simulations," GE Power Systems Energy Consulting, IEEE WTG Modeling Panel, Session July 2003.

[20] Sun, T., Chen, Z., and Blaabjerg, F., "Flicker Study on Variable Speed Wind Turbines with Doubly Fed Induction Generators," *IEEE Transactions on Energy Conversion*, vol. 20, no. 4, pp. 896-905, December 2005.

[21] Morren, J., and de Haan, S.W.H., "Ridethrough of wind turbines with doubly-fed induction generator during a voltage dip," *IEEE Transactions on Energy Conversion*, vol. 20, no. 2, pp. 435-441, June 2005.

[22] Lei, Y., Mullane, A., Lightbody, G., and Yacamini, R.,"Modeling of the Wind Turbine with a Doubly Fed Induction Generator for Grid Integration Studies," *IEEE Transactions on Energy Conversion*, vol. 21, no. 1, pp. 257-264, March 2006.

[23] Polinder, H., van der Pijl, F.F.A., de Vilder, G.J., and Tavner, P.J., "Comparison of Direct-Drive and Geared Generator Concepts for Wind Turbines," *IEEE Transactions on Energy Conversion*, vol. 21, no. 3, pp. 725-733, September 2006.

[24] Morren, J., and de Haan, S.W.H., "Short-Circuit Current of Wind Turbines with Doubly Fed Induction Generator," *IEEE Transactions on Energy Conversion*, vol. 22, no. 1, pp. 174-180, March 2007.

[25] Szabó, L., Biró, K.Á., Cosmina, N., and Jurca, F., "Dynamic Simulation of Induction Generators Coupled to Wind Turbines," *Proceedings of the 11th IEEE International Conference on Intelligent Engineering Systems* (INES '2007)2007.

[26] Beltran, B.; Ahmed-Ali, T.; El Hachemi Benbouzid, M. Sliding mode power control of variable-speed wind energy conversion systems. *IEEE Trans. Energy Conversion*. Vol. 23, 551–558, 2008,.

[27] Pao, L.; Johnson, K. A Tutorial on the Dynamics and Control of Wind Turbines and Wind Farms. *In Proceedings of the American Control Conference*, 10–12 June 2009; pp. 2076–2089.

[28] Jonkman, J.M., Butterfield, S., Musial,W., Scott, G., "Definition of a 5-MW Reference Wind Turbine for Offshore System Development", Technical Report NREL/TP, National Renewable Energy Laboratory: Golden, CO, USA, 2009.

[29] Beltran, B.; Ahmed-Ali, T.; Benbouzid, M. High-order sliding-mode control of variable-speed wind turbines. *IEEE Trans. Ind. Electr*. vol.56, 3314–3321, 2009.

[30] Soliman, M., Malik, O.P., Westwick, D.T., "Multiple Model MIMO Predictive Control for Variable Speed Variable Pitch Wind Turbines", *In Proceedings of the American Control Conference*, June–2 July 2010.

[31] Khezami, N.; Braiek, N.B.; Guillaud, X. "Wind turbine power tracking using an improved multimodel quadratic approach," *Int.Soc. Autom. Trans*., vol. 49, 326–334, 2010.

[32] Acho, L.; Vidal, Y.; Pozo, F. Robust "variable speed control of a wind turbine," *Int. J. Innov. Comput. Inf. Control*, vol. 6, 1925–1933, 2010.

[33] Kusiak, A., Zhang, Z., "Control of wind turbine power and vibration with a data-driven approach," *Renew. Energy* vol. 43, pp. 73–82, 2012.

[34] Hassan, H.M., Eishafei, A.L., Farag, W.A., Saad, M.S., "A robust LMI-based pitch controller for large wind turbines," *Renew. Energy*, vol. 44, pp. 63–71, , 2012.

[35] Sandquist, F., Moe, G.; Anaya-Lara, O., "Individual pitch control of horizontal axis wind turbines," *J. Offshore Mech. Arctic Eng.-Trans. ASME*, vol. 134, , 2012.

[36] Joo, Y., Back, J., "Power regulation of variable speed wind turbines using pitch control based on disturbance observer," *J. Electr. Eng. Technology*, vol. 7, pp. 273–280, 2012.

[37] Diaz de Corcuera, A., Pujana-Arrese, A., Ezquerra, J.M., Segurola, E., Landaluze, J., "H-infinity based control for load mitigation in wind turbines", *Energies*, vol. 5, pp. 938–967, 2012.